NANO LETTERS

Letter

pubs.acs.org/NanoLett

Spin Orientation of Two-Dimensional Electrons Driven by Temperature-Tunable Competition of Spin−Orbit and Exchange−Magnetic Interactions

Alexander Generalov,[†] Mikhail M. Otrokov,[‡,§] Alla Chikina,[⊥] Kristin Kliemt,[¶] Kurt Kummer,[#] Marc Höppner,[∥] Monika Güttler,[⊥] Silvia Seiro,[□] Alexander Fedorov,[○] Susanne Schulz,[⊥] Steffen Danzenbächer,[⊥] Evgueni V. Chulkov,[‡,§,△] Christoph Geibel,[□] Clemens Laubschat,[⊥] Pavel Dudin,[■] Moritz Hoesch,[■] Timur Kim,[■] Milan Radovic,[●,▲] Ming Shi,[●] Nicholas C. Plumb,[●] Cornelius Krellner,[¶,*] and Denis V. Vyalikh[*,‡,⊥,^,△]

[†]MAX IV Laboratory, Lund University, Box 118, 22100 Lund, Sweden

[‡]Departamento de Fisica de Materiales and CFM-MPC UPV/EHU, Donostia International Physics Center (DIPC), 20080 San Sebastian, Spain

[§]Tomsk State University, Lenina Av., 36, 634050 Tomsk, Russia

[⊥]Institute of Solid State Physics, Dresden University of Technology, Zellescher Weg 16, D-01062 Dresden, Germany

[¶]Kristall- und Materiallabor, Physikalisches Institut, Goethe-Universität Frankfurt, Max-von-Laue Straße 1, D-60438 Frankfurt am Main, Germany

[#]European Synchrotron Radiation Facility, 71 Avenue des Martyrs, CS40220, F-38043 Grenoble Cedex 9, France

[∥]Max Planck Institute for Solid State Research, Heisenberg Straße 1, D-70569 Stuttgart, Germany

[□]Max Planck Institute for Chemical Physics of Solids, Nöthnitzer Straße 40, D-01187 Dresden, Germany

[○]IFW Dresden, P.O. Box 270116, D-01171 Dresden, Germany

[△]Saint Petersburg State University, 198504 Saint Petersburg, Russia

[■]Diamond Light Source, Didcot OX11 0DE, U.K.

[●]Swiss Light Source and [▲]SwissFEL, Paul Scherrer Institute, CH-5232 Villigen-PSI, Switzerland

[^]IKERBASQUE, Basque Foundation for Science, 48011 Bilbao, Spain

Supporting Information

ABSTRACT: Finding ways to create and control the spin-dependent properties of two-dimensional electron states (2DESs) is a major challenge for the elaboration of novel spin-based devices. Spin−orbit and exchange−magnetic interactions (SOI and EMI) are two fundamental mechanisms that enable access to the tunability of spin-dependent properties of carriers. The silicon surface of $HoRh_2Si_2$ appears to be a unique model system, where concurrent SOI and EMI can be visualized and controlled by varying the temperature. The beauty and simplicity of this system lie in the 4*f* moments, which act as a multiple tuning instrument on the 2DESs, as the 4*f* projections parallel and perpendicular to the surface order at essentially different temperatures. Here we show that the SOI locks the spins of the 2DESs exclusively in the surface plane when the 4*f* moments are disordered: the Rashba-Bychkov effect. When the temperature is gradually lowered and the system experiences magnetic order, the rising EMI progressively competes with the SOI leading to a fundamental change in the spin-dependent properties of the 2DESs. The spins rotate and reorient toward the out-of-plane Ho 4*f* moments. Our findings show that the direction of the spins and the spin-splitting of the two-dimensional electrons at the surface can be manipulated in a controlled way by using only one parameter: the temperature.

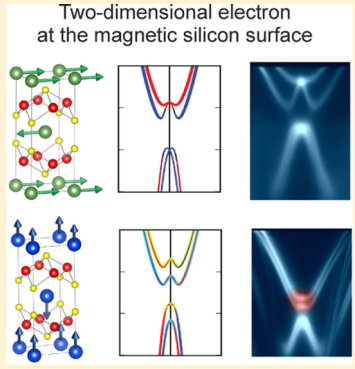

KEYWORDS: *Spin−orbit coupling, exchange−magnetic interaction, rare-earth intermetallics, antiferromagnetism, ARPES*

Controlling the spin orientation as well as the spin-splitting of electronic states at surfaces and interfaces is the major challenge for spintronics that rely on the spin of electrons.[1] There are two fundamental mechanisms that allow to create

Received: September 27, 2016
Revised: December 22, 2016
Published: December 29, 2016

DOI: 10.1021/acs.nanolett.6b04036
Nano Lett. 2017, 17, 811−820

spin-polarized properties: spin−orbit and exchange−magnetic interactions (SOI and EMI). The possibility to obtain spin-polarized electron states without an external magnetic field and solely due to spin−orbit coupling was first seen for bulk semiconductors with zinc blende crystal structures and explained by an absence of inversion symmetry in the crystal structure.[2] Later on, it was shown by Rashba and Bychkov that in two-dimensional (2D) systems like semiconductor quantum wells or surfaces of solids, the spin degeneracy can be lifted as well due to a lack of inversion symmetry at interfaces, which is now known as the Rashba−Bychkov (RB) effect.[3,4] This has generated a lot of interest and a quest for more classes of materials where similar properties can be envisaged and tuned in a controlled way.[5] The pronounced effect was observed for 2D states present at surfaces of various metals, oxides, and topological insulators.[5−14] Besides, an analogous effect was reported for the three-dimensional (3D) bulk states of systems without bulk inversion symmetry, which coexists with the RB effect of 2D states at their surfaces.[15−18] Recent studies have indicated the fascinating opportunities for spin-dependent transport of the room-temperature ferroelectric semiconductor GeTe, in which the coexistent RB-type surface state and a spin-polarized helical bulk state at the Fermi level can be switched and modulated in spin direction by nonvolatile control of the ferroelectric polarization.[19−21]

Note that spin transport effects induced solely by SOI are rather subtle and often detected only indirectly in electrical transport measurements.[22,23] To produce sizable spin transport effects in RB systems, different strategies were proposed that introduce spin-asymmetry involving exchange interactions. One of them is to induce spin-mixing by applying an external magnetic field in the direction transverse to the effective magnetic field induced by RB effect.[22] Another example of exploiting exchange interaction to control the spin-polarization in systems with a RB effect has been recently reported for thin films of Ag_2Bi grown on ferromagnetic Fe(110) substrates.[24] There, the concurrent lack of inversion and time reversal symmetry due to an in-plane magnetic field gives rise to asymmetric gap openings in the quantum-well states of Ag_2Bi. Model transport calculations reported in that study reveal the importance of such asymmetries for spin-polarized transport.

The action of both spin−orbit and exchange−magnetic interactions is responsible for many intriguing phenomena in condensed matter. The prominent examples are the quantum spin and anomalous Hall effects in topological insulators.[23,25−30] Magnetic proximity coupling with a ferromagnetic (FM) or antiferromagnetic (AFM) insulator[31,32] or magnetic impurity[33] allows the surface states of topological insulators to experience ferromagnetic interactions and makes it possible to observe exotic phenomena like the predicted topological magnetoelectric effect.[34] The recently reported robust magnetism at the interface of $LaAlO_3/SrTiO_3$[11,12] as well as discussable properties at the surface of native $SrTiO_3$ is a further curious example.[13,14] Another important class of materials where both types of interactions play a crucial role are materials known as "frustrated magnets" or "magnetic ferroelectrics" where ferroelectricity is induced by magnetic ordering.[35] Just recently, it has been shown for the multiferroic $Ge_{1-x}Mn_xTe$ that the spin helicity of the RB bands can be effectively switched to the opposite by the magnetic field reversal as a consequence of inherent entanglement of magnetic and spin−orbit order.[36] All these examples clearly demonstrate the huge potential of materials where unusual electronic and magnetic properties are handled by SOI and EMI. At present, AFM materials seem the most promising candidates for spintronic applications due to their capability of producing large magneto-transport effects in combination with robustness against perturbation by magnetic fields and the absence of parasitic stray fields allowing for a reduced power consumption and size of respective devices.[37]

Here, we demonstrate that the spin properties of two-dimensional electron states trapped at the Si-terminated surface of $HoRh_2Si_2$ are dictated by SOI and EMI and can be controlled by temperature without the need of an external magnetic field. Like in several other $RERh_2Si_2$ compounds, the magnetic structure of $HoRh_2Si_2$ is composed of ferromagnetic Ho layers in the *ab*-planes stacking AFM to each other along the *c* axis and separated by Si−Rh−Si trilayers. The unique property of this antiferromagnet is that the in-plane and out-of-plane components of the Ho 4*f*-moments order at notably different temperatures. Together with the RB SOI, this results in effective magnetic fields with different strength and orientation, which act on the highly mobile two-dimensional electrons locked within the outermost Si−Rh−Si trilayer, leading to a temperature-dependent spin-polarization. Applying angle-resolved photoelectron spectroscopy (ARPES),[38] we show that in the paramagnetic (PM) phase, above ∼29.5 K, where the Ho 4*f* moments (further also referred to as 4*fs*) are disordered, the spin-splitting of the Shockley 2DES is driven by RB SOI. It forces the spins of the Shockley electrons to be aligned within the surface plane. When the temperature is gradually lowered below the Néel temperature, the Ho 4*f* moments create a ferromagnetic layer underneath the silicon surface. First, the 4*fs* component perpendicular to the surface becomes ordered. The long-range order increases the magnitude of the exchange−magnetic interaction between the 4*f* moments and the itinerant surface electrons. Dominating over RB SOI, the rising EMI leads to changes in the spin-splitting of the Shockley state and to realignment of the spins. It forces them to abandon their in-plane orientation and align along the direction of the ordered Ho 4*f* moments. With a further decrease in temperature, the 4*f* moments component parallel to the surface plane becomes ordered. Consequently, this leads to their tilting, modifying the effective magnetic field at the surface and, as a result, the spin-dependent properties of the Shockley state. Our experimental and theoretical results allow us to disclose and show in detail how the combination of RB SOI and EMI in one system allows manipulating the three-dimensional direction of the spin and the energy of 2DESs in a controlled way by changing only one parameter: the sample temperature. This toy model system can be considered as a promising playground for elaboration of novel electronic, ferroelectric, and especially Si-based spintronic devices where both spin−orbit and exchange−magnetic interactions can be combined.[39,40]

Properties of Two-Dimensional Rashba-like Electrons in Internal Magnetic Fields: Out-of-Plane versus in-Plane Orientation of 4*f* Moments. Our system is a silicon terminated single crystal of $HoRh_2Si_2$, which exhibits antiferromagnetic ordering at low temperatures with a rather curious property, a so-called "successive component-separated magnetic transition".[41] This basically means that the components of Ho 4*f* moments that are parallel and perpendicular to the surface plane order at different temperatures. $HoRh_2Si_2$ possesses a layered structure of $ThCr_2Si_2$ type where Ho atomic layers are separated by strongly bonded Si−Rh−Si blocks along the [001] direction.[42]

DOI: 10.1021/acs.nanolett.6b04036
Nano Lett. 2017, 17, 811−820

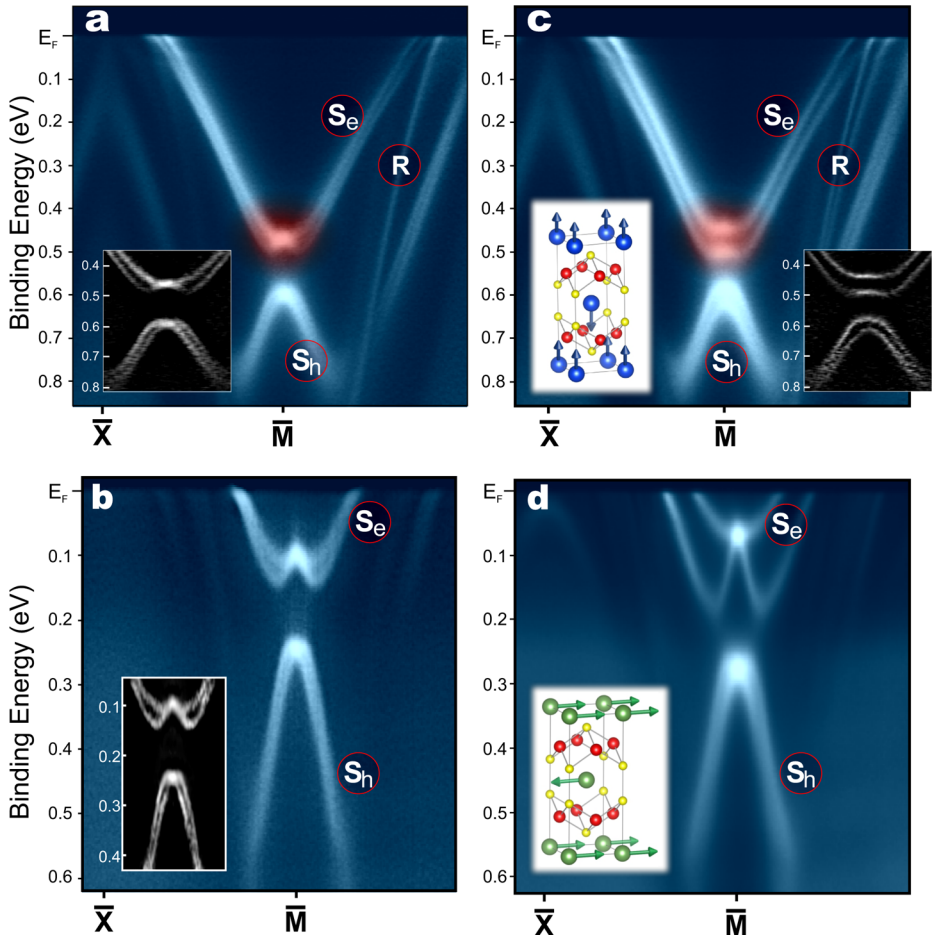

Figure 1. ARPES intensity maps measured along the $\bar{X}-\bar{M}-\bar{X}$ direction for $HoRh_2Si_2$ (a,c) and $EuRh_2Si_2$ (b,d) above (a,b) and below (c,d) the corresponding transition into the AFM ordered state. Insets on panels a and b show the second derivatives of the respective ARPES maps in the vicinity of the $\bar{M}$-point. The data for $HoRh_2Si_2$ were obtained at 40 K (a) and 15 K (c), whereas for $EuRh_2Si_2$ at 55 K (b) and 10 K (d). The insets at the bottom left of panels c and d show the corresponding unit cells with the direction of 4*f* moments on rare earth atoms indicated by arrows. Yellow (red) balls correspond to Si (Rh) atoms.

In detail, the magnetic order of the system develops as follows. The transition from the paramagnetic to a simple antiferromagnetic state occurs in a two-step process with a second order type transition at ∼29.5 K followed by a first order transition at a slightly smaller temperature ∼27 K.[41] The intermediate phase is not well-studied and has been proposed to be an incommensurate magnetic structure.[41] Below 27 K, the magnetic structure is a simple commensurate one with ferromagnetic *ab*-planes stacked as "+-+-" along the *c*-direction.[41,43] However, analysis of experimental results indicates that at 27 K only the *c*-component of the 4*f* moments orders.[41,44] In the following, we will refer to this phase as AFM-I with the bulk Néel temperature, T_{N1}, equal to 27 K. At 12 K, one observes a further, well-defined second order type thermodynamic transition, with a large anomaly in the specific heat.[41,44] Analysis of the experimental results indicate that this transition corresponds to the ordering of the in-plane component of the 4*f* moment.[41,44] This results in a tilting of the staggered AFM moment away from the tetragonal axis, up to an angle of about 28° at 4 K.[41,43] We will refer to this antiferromagnetic phase as AFM-II with a T_{N2} of 12 K. At low *T*, the magnitude of the ordered moment, about 9.5 μ_B, is close to the saturation moment of 10 μ_B expected for the $^5I_8$, $J = 8$ ground state multiplet of Ho.[43] Thus, at 4 K, the *c*-component of the 4*f* ordered moment amounts to about 8.3 μ_B, while the in-plane component is about 4.1 μ_B. Note that this property is in remarkable difference to that of antiferromagnets $EuRh_2Si_2$ and $GdRh_2Si_2$, where the 4*f* moments lie exclusively in the *ab*-plane.[45,46]

This kind of transition, which is also called "spin reorientation transition" is quite common in heavy RE systems. It results from a competition between low and high order crystal electric field (CEF) parameters.[47] At high *T*, the excited CEF levels are thermally populated and therefore only the lowest order CEF-parameter (B_2^0) is effective. In case of $HoRh_2Si_2$, it forces the moment to order along the *c*-direction.[44] With decreasing *T*, higher order CEF parameter becomes more and more relevant. In case of $HoRh_2Si_2$ the next order CEF parameter (B_4^0) promotes a tilting by 45°. Competition of both CEF parameters leads to the observed tilting angle of about 28°.[44,48]

We will show now that this peculiar out-of-plane bulk magnetic order in $HoRh_2Si_2$ gives rise to surface magnetic and electronic properties very different to those of its in-plane ordered homologues, like $EuRh_2Si_2$ or $GdRh_2Si_2$. Figure 1 shows ARPES intensity maps taken along the $\bar{X}-\bar{M}-\bar{X}$ direction of the surface Brillouin zone (SBZ) of the Si-terminated $HoRh_2Si_2$ and $EuRh_2Si_2$ systems for both the PM and AFM phases. We begin with discussion of the ARPES data in the PM case (Figures 1a and 1b) before looking at the

DOI: 10.1021/acs.nanolett.6b04036
Nano Lett. 2017, 17, 811−820

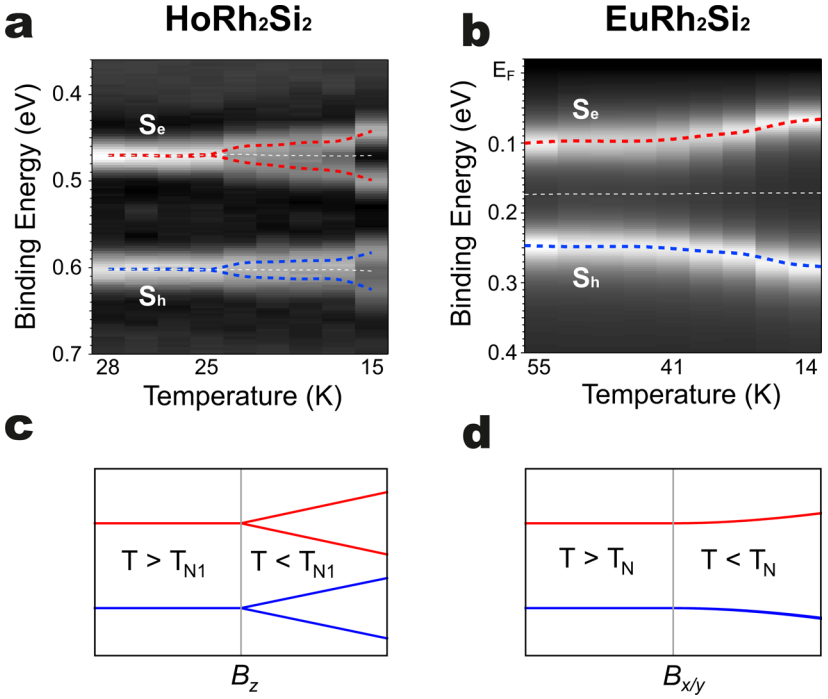

Figure 2. Photoemission intensity for EDC at the $\bar{M}$-point as a function of temperature for (a) $HoRh_2Si_2$ and (b) $EuRh_2Si_2$ and calculated energy splitting of the tight binding model for an out-of-plane (c) and an in-plane (d) magnetic field. Red- and blue-colored lines correspond to electron- and hole-like states at the $\bar{M}$-point, respectively. The dashed white lines in panels a and b correspond to the center of gravity of the corresponding split bands. Note that the temperature scale on the figures is not linear.

changes when the two systems are cooled into the magnetically ordered state. The most prominent feature in the ARPES maps is a Shockley surface state,[6] that is, a two-dimensional electron state that is trapped at the silicon surface of these compounds.[45,46] The estimation of the Fermi velocity suggests that it is about 1.2×10^5 m/s in the Ho- and 1.7×10^5 m/s in the Eu-based materials, indicating a highly mobile character of these two-dimensional electrons. The Shockley state consists of electron-like (S_e) and hole-like (S_h) partners located in the projected bulk band gap centered at the $\bar{M}$-point. Evidently, it is found at a notably higher binding energy (BE) in $HoRh_2Si_2$ than in $EuRh_2Si_2$. This is a direct consequence of the trivalence of the Ho ions (Ho^{3+}) as compared to the divalent Eu ones (Eu^{2+}) in $EuRh_2Si_2$, which raises the Fermi level to accommodate the additional Ho 5*d* valence electron (see also Supplementary Note 5).

Close inspection of Figures 1a and 1b shows that at the $\bar{M}$-point the electron- and hole-like counterparts are well separated by a noticeable gap of about 130 and 150 meV for $HoRh_2Si_2$ and $EuRh_2Si_2$ systems, respectively. In addition to that, there is also a notable ***k***-dependent splitting of the S_e and S_h partners, which disappears exactly at the $\bar{M}$-point leading to a two-fold degeneracy of the S_e and S_h states there. This can be explicitly seen in the respective insets, where the second derivative of the experimental ARPES data near the $\bar{M}$-point is shown. The observed energy splitting at the $\bar{M}$-point together with the ***k***-dependent splitting of the S_e and S_h bands can be well understood and explained as a result of two types of spin−orbit effects acting on the Shockley electrons. Note that without SOI, the spin-degenerate electron- and hole-like states would touch each other at the $\bar{M}$-point resulting in a four-fold degenerate electron state, see ref 45 and Supplementary Figure S1a.

The first effect is a splitting of the states at the $\bar{M}$-point by pure or intrinsic SOI[49] (Supplementary Figure S1b), which lifts the four-fold degeneracy of the states at the $\bar{M}$-point. The second effect is the RB effect, which acts on the two-dimensional electron state as a consequence of the breaking of inversion symmetry at the crystals surface. It lifts the spin-degeneracy of both bands except for the $\bar{M}$-point where the spin-split states cross as seen in Figure 1a and b (see also Supplementary Figure S1c). Thus, SOI leads to strong ***k***-dependent spin-mixing in the vicinity of the crossing point $\bar{M}$ (Supplementary Figure S1b). However, by moving away from the high-symmetry point along the electron-like state and coming closer to the Fermi level, the spin polarization of each spin-split band increases. Moreover, because of the RB effect, the spins of the Shockley state are locked within the *ab*-plane (Supplementary Figure S1c). Thus, at the Fermi level the spins of the Shockley electrons in both $HoRh_2Si_2$ and $EuRh_2Si_2$ will be aligned exclusively within the surface *ab*-plane for temperatures where 4*f*-derived magnetism is not yet developed.

The properties of the two-dimensional electrons will be significantly modified when both systems $EuRh_2Si_2$ and $HoRh_2Si_2$ will become AFM ordered. We will see that below the Néel temperature, the exchange−magnetic interaction has a remarkably striking and rather different effect on the Shockley state in these systems. Inspection of Figure 1c and d allows to conclude that first, the spin-splitting over the whole Brillouin zone is increased for the 2DESs of both systems. This is because of the exchange interaction of the Shockley state spins with the ordered 4*f* moments of the corresponding RE ions. The noticeably larger splitting in the $EuRh_2Si_2$ relates to the larger pure spin moment of Eu^{2+} ions of about 7 μ_B[45,50] compared to about 4 μ_B spin moment of Ho^{3+} ions in $HoRh_2Si_2$.[43,51,52] However, while the spin-degeneracy of both the electron- and hole-like parts of the Shockley surface states at the $\bar{M}$-point survives in $EuRh_2Si_2$ (Figure 1d), it is fully lifted in $HoRh_2Si_2$ (see Figure 1c and Supplementary Figure S1d). As

DOI: 10.1021/acs.nanolett.6b04036
Nano Lett. 2017, 17, 811−820

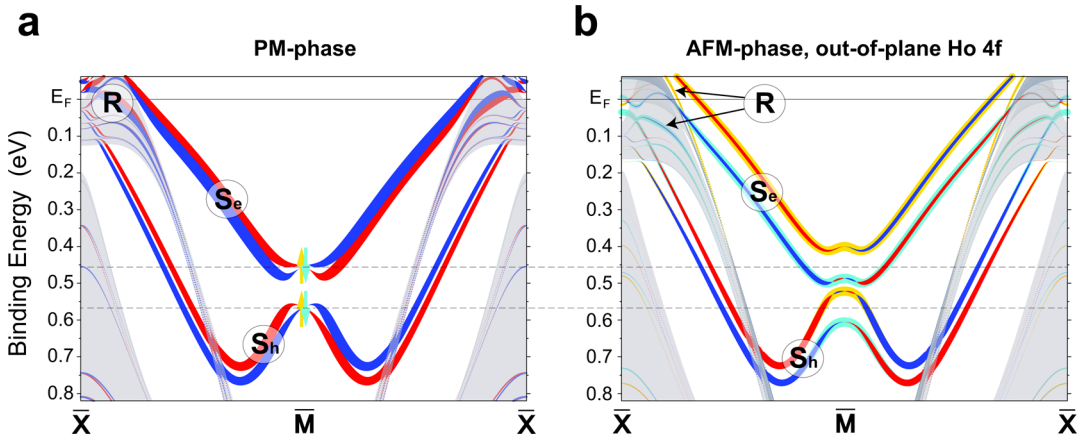

Figure 3. Spin-resolved surface band structure calculations along the $\bar{X}-\bar{M}-\bar{X}$ path in the SBZ of $HoRh_2Si_2$ in the PM phase (a) and the AFM-I phase (b) (the 4*f* moments are aligned along the surface normal). The red and blue color indicate the opposite in-plane $S_{x,y}$ spin-components. Yellow and cyan colors stand for out-of-plane $+S_z$ and $-S_z$ spin-components, respectively. The width of the lines translates into the contribution of the first four surface atomic layers Si−Rh−Si−Ho to the spin polarization.

a consequence, we observe a surface state split into four distinct bands: two electron-like and two hole-like that can be clearly seen in Figure 1c. Note that band-structure modifications similar to the $EuRh_2Si_2$ case with remaining spin-degeneracy at the $\bar{M}$-point have been recently reported by us for the trivalent compound $GdRh_2Si_2$ in the AFM phase.[46]

As known from bulk-sensitive measurements, the principal difference of $HoRh_2Si_2$ to its structural homologues $EuRh_2Si_2$ and $GdRh_2Si_2$ is the alignment of the ordered 4*f* moments. In $HoRh_2Si_2$, it is along the *c*-direction below the T_{N1} of 27.2 K,[43] that is, perpendicular to the surface, whereas in the Eu- and Gd-based compounds it is exclusively in *ab*-plane.[42,50,53,54]

Thus, the obvious question is whether the observed differences in the band-structure modifications in $HoRh_2Si_2$ and $Eu(Gd)Rh_2Si_2$ can be caused by different magnetocrystalline anisotropies.

For a pure RB SOI system, it has been known for several decades that an external magnetic field transversal to the surface lifts the spin-degeneracy at the parabolas crossing point.[4,55] A similar effect of symmetric band gap opening has also been recently reported for the surface states in topological insulators due to Mn magnetic impurities magnetized perpendicular to the sample surface.[33] In addition, it has just recently been shown that a collinear alignment of the ferroelectric polarization and magnetization in multiferroic $Ge_{1-x}Mn_xTe$ leads to an opening of a Zeeman gap of up to 100 meV at the crossing point of the RB bands.[36]

Qualitatively, the conserved spin-degeneracy near the $\bar{M}$-point in Eu system can be explained as follows. When the 4*f* moments are disordered, then only the RB SOI defines the spin-splitting of the Shockley states except at the $\bar{M}$-point and their spins are locked within the *ab*-plane. At the $\bar{M}$-point, both S_e and S_h bands remain two-fold degenerate due to the vanishing RB field. Now, when an external, additional in-plane magnetic field develops due to ordering of the 4*f* moments, it simply adds to the effective RB field, still keeping the electron spins within the *ab*-plane. Description of this 4*f*-derived magnetic field can be added to the RB Hamiltonian. As a consequence, two-fold degeneracy for both S_e and S_h bands will remain (Supplementary Figure S1).

For $HoRh_2Si_2$, the situation is principally different because there is an exchange−magnetic interaction due to the *c*-directed magnetic field. This interaction will lift the remaining two-fold spin degeneracy at the $\bar{M}$-point and determine the EMI-derived splitting of the S_e and S_h bands at this point.[33,36] The latter can be nicely seen in ARPES-derived spectral pattern shown in Figure 1c. We will later see that the observed band structure modifications in $HoRh_2Si_2$ are fully reproduced by ab initio and model band structure calculations (Supplementary Notes 1 and 2; Figures S1 and S2).

To get further insight into the nature of the observed band-splitting at the $\bar{M}$-point in $HoRh_2Si_2$, we show in Figure 2 the energy distribution curves (EDCs) of the photoemission intensity as a function of temperature for $HoRh_2Si_2$ (a) and $EuRh_2Si_2$ (b). A series of temperature-dependent measurements spans the region around the Néel temperature T_N = 24.5 K in $EuRh_2Si_2$[50] and the first transition temperature of $HoRh_2Si_2$ T_{N1} at 27 K. Well above the transition temperatures, in the PM phase, the situation is rather similar for both materials: a pair of intensity maxima is observed, which corresponds to the electron- and hole-like spin-degenerate Shockley surface states at the $\bar{M}$-point (Figure 2a,b). In the case of $HoRh_2Si_2$, when the temperature lowers below ∼25 K, a Zeeman-like splitting can be clearly observed for both electron- and hole-like partners and is captured as well by our model calculation (see Figure 2c). The linear dependence of the energy difference on the 4*f* magnetic moment can be derived from our tight binding model calculations, see Supplementary Note 4 and Figure S6. The measured onset of splitting in $HoRh_2Si_2$ is significantly lower than the bulk T_{N1} of 27 K,[41] which can be understood in terms of weaker exchange interaction due to smaller coordination numbers of magnetic ions at the surface of the crystal.[46,56]

The temperature-dependent data for $EuRh_2Si_2$, where the 4*f* moments order within the *ab*-plane, that is, parallel to the surface, reveal remarkably different behavior (Figure 2b). No splitting is observed either for electron- or hole-like states across the entire temperature range, while the energy gap between the electron- and hole-like states increases with decreasing temperature. In our tight binding model, the electron and hole-like states show a similar behavior as a function of the 4*fs* magnetic field and do not significantly split (see Figure 2d). The difference between $EuRh_2Si_2$ and $HoRh_2Si_2$ in the temperature evolution of the electronic states at the $\bar{M}$-point originates from SOI in combination with the induced magnetization by the 4*f* moments field as well as the

DOI: 10.1021/acs.nanolett.6b04036
Nano Lett. 2017, 17, 811−820

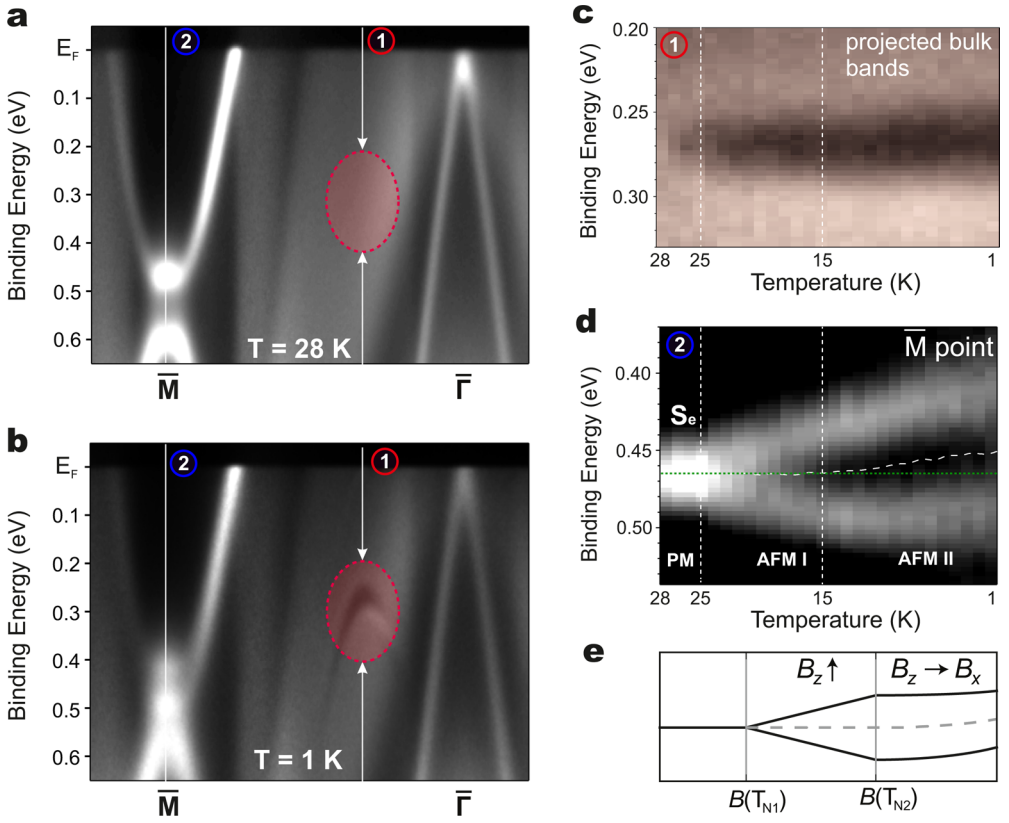

Figure 4. ARPES derived band map taken along the $\bar{\Gamma}$–$\bar{M}$ direction at (a) T = 28 K and (b) 1 K, respectively. The red-dashed ellipse indicates the region where the splitting of the bulk projected bands is developed below 27 K. (c) Temperature-dependence of the EDC labeled as (1) in panels a and b. (d) Temperature-dependence of the spin-splitting of the electron-like state S_e at the $\bar{M}$-point of the SBZ down to 1 K. The center of gravity of both lines is shown by dashed white line. (e) Calculated splitting of the electron-like state of the tight binding model at the $\bar{M}$-point of the SBZ as a function of the strength as well as the direction of the magnetic field. The center of gravity is indicated by a gray dashed line.

surface potential, see Supplementary Figures S1, S2, S6 and Note 4. In the Ho compound, the magnetic moments point along the surface normal, parallel to the surface potential gradient. By contrast, in the Eu compound, the magnetic moments lie in the plane and are thus perpendicular to the surface potential gradient. Since to first order $\boldsymbol{L}$ is the same in both compounds, the effect of SOI, that is, $\boldsymbol{L}\cdot\boldsymbol{S}$, in the magnetically ordered phase has to be different, see Supplementary Figures S1, S2, S6–S8, and Note 4.

To explain the experimental results above, we have performed ab initio electronic structure calculations of the (001)-surface of $HoRh_2Si_2$ taking into account both SOI and EMI. The calculated band structure along $\bar{X}$–$\bar{M}$–$\bar{X}$ is presented in Figure 3. It can be seen that the band structure calculated for the $HoRh_2Si_2$ paramagnetic phase (Figure 3a) reproduces very well the overall experimental band structure shown in Figure 1a. Moreover, the calculated largest value of the spin-splitting of the electron-like state S_e of 35 meV agrees perfectly with the experimental value of about 35 meV. In general, the band dispersions obtained theoretically reveal RB-like behavior for both electron- and hole-like states (S_e and S_h). This can be clearly seen in the spin textures they feature: the positive and negative spin branches are shifted in opposite $\boldsymbol{k}$-directions, spin vectors are lying within the *ab*-plane and are locked perpendicular to the momentum in the vicinity of the $\bar{M}$-point. Close to the $\bar{M}$-point, there is a deviation from the RB-like effect. The SOI, which couples the electron- and hole-like state, introduces a spin-mixing by manifesting itself in a pronounced decrease of the spin expectation value as shown by the diminishing width of the red and blue lines in Figure 3a. However, despite the spin-mixing, the spin moments still lie in the *ab*-plane (except for the $\bar{M}$-point). It is important to note that at the $\bar{M}$-point the spin polarization of both, the electron- and hole-like states, have well-defined out-of-plane directions of opposite signs as shown by vertical yellow and cyan arrows (Figure 3a). This result straightforwardly implies that if an external magnetic field was introduced perpendicular to the Si-terminated surface of $HoRh_2Si_2$, the degenerate states would split to first order in a Zeeman-like fashion, that is, symmetrically with respect to the energy of unsplit states.[33,36] This is exactly what we observe in the temperature-dependent ARPES data for $HoRh_2Si_2$ in Figure 2a. Thus, below the temperature of 25 K, the Ho 4*f* moments in the subsurface layer become ordered along the *c*-direction, that is, in the same way as in bulk.

To theoretically interpret the ARPES image acquired for $HoRh_2Si_2$ at 15 K (Figure 1c), we have performed slab calculations for the AFM-I phase in which the Ho 4*f* moments are oriented perpendicular to the surface. The corresponding results are shown in Figure 3b. In agreement with the experiment, the spin-degeneracy of the Shockley states at the $\bar{M}$-point is lifted and the spin-splitting away from the point increases with respect to that in the paramagnetic phase (cf. Figure 3a). We note, however, that the calculation yields a notably larger spin-splitting for the electron-like state at the $\bar{M}$-point − 87 meV against approximately 56 meV measured at 15 K. Analysis of the T dependence of the 4*f* entropy shows that a large part of the CEF split states of the $^5I_8$ J = 8 ground state

DOI: 10.1021/acs.nanolett.6b04036
Nano Lett. 2017, 17, 811–820

multiplet are involved in the formation of the AFM state, indicating the overall CEF splitting to be only slightly larger than T_{N1}.[41,44] An extrapolation of the experimental splitting magnitudes, obtained in the range from 40−15 K (Figure 2a), down to 0 K by the Weiss mean-field magnetization curve with total angular momentum $J = 8$,[46,56] gives saturation values for the splitting of about 65 ± 4 meV, which is still significantly smaller than the calculated value. In the next section we show by our temperature dependent measurements down to 1 K and slab calculations that the discrepancy at very low temperatures is nicely lifted by assuming a tilt for 4*f* moments in the calculation with respect to the surface normal.

Further, it should be noted that the calculations indicate the drastic changes in the whole spin-texture of the Shockley states. We observe a strong out-of-plane spin component for the overall structure of the surface states up to the Fermi level which are, in most of the cases, even overcome the absolute value of the in-plane ones (Figure 3b). That leads to the remarkable conclusion that as a result of the quite specific combined action of concurrent SOI and EMI in $HoRh_2Si_2$ the spins of the 2DESs undergo rotations gradually turning out of the *ab*-plane toward the direction of the surface normal as the temperature goes down.

2DESs in a Tilted Magnetic Field. We turn now to the discussion on how the temperature-separated order of the 4*f*s projections perpendicular and parallel to the surface is reflected in the spin-dependent properties of 2DESs. Note that in the bulk they become ordered at 27 and 12 K, respectively. For that, we have extended our temperature-dependent ARPES measurements down to 1 K and precisely explored the evolution of the spectral pattern along the $\bar{\Gamma}-\bar{M}$ direction focusing on the vicinity of the $\bar{M}$-point. The respective results are shown in Figure 4a−d. Our experiments allow us first to detect the splitting of the projected bulk bands, which are visible within the red-dashed ellipse in Figure 4b. The analysis of its temperature evolution, shown in Figure 4c, indicates an onset point as 27 K. This agrees well with the known bulk T_{N1} determined from macroscopic bulk-sensitive measurements.[41,43] The slab calculations along the $\bar{\Gamma}-\bar{M}$ direction also reveal a pair of the exchange-split surface resonances located in the same energy and momentum region (Supplementary Figure S3).

We focus now on the temperature behavior of the Shockley state split at the $\bar{M}$-point (Figure 4d). As we have discussed just above, between 25 and 15 K, the splitting develops "symmetrically" with respect to the maximum of PE intensity of the unsplit band measured in the PM phase and marked by the green dotted line. Note that the full-width at half-maximum of the unsplit band S_e above 25 K is almost constant and is slightly less than those of the spin-split bands at $T = 15$ K. This implies that at temperatures higher than 25 K, the splitting should be explicitly considered to be vanishing (or zero) in full agreement with the analysis above. However, when the temperature decreases below ∼15 K, one can see a steady shift of the center of gravity of the spin-split bands to higher energies, which is shown by the dashed white line in Figure 4d. The asymmetry of the splitting can be clearly seen. The maximum deviation of the center of gravity from the position in the PM phase reaches a value of 15 meV at 1 K. Curiously, such an evolution of the $HoRh_2Si_2$ electron-like surface state below 15 K is reminiscent of that seen for the degenerate S_e band of $EuRh_2Si_2$ (Figures 2b and 2d). There, the latter was explained by the occurrence of an effective in-plane magnetic field due to the ordered Eu 4*f* moments. Thus, it is appealing to link the observed changes in the Ho-based system to the onset of a nonzero in-plane magnetic 4*f* moment. This means that the in-plane component of the 4*f* moments becomes ordered, or in other words, the Ho 4*f* moments get tilted with respect to the surface normal already at the temperature of 15 K. This marks the onset of an in-plane effective magnetic field, which together with the much stronger field perpendicular to the surface will affect the spin properties of the Shockley state. Interestingly, this onset temperature is slightly larger than the bulk $T_{N2} \approx 12$ K.[41] Our interpretation is further supported by ab initio and model calculations, performed for different tilts of Ho^{3+} 4*f* moments, see Figure 4e and Supplementary Figures S1, S2, and S4 and Note 2. For the tilt angle of 28° out of the vertical axis, the first-principles calculation yields a 14-meV-shift for the center of gravity of the spin-split states S_e at the $\bar{M}$-point (Supplementary Figure S4) with respect to the nontilted case, which agrees nicely with the above given experimental value of 15 meV. Besides, the respective saturated value of the spin-splitting of 72.5 meV derived from the slab-calculations for the tilt angle of 28 degree (Supplementary Figure S4) is in very good agreement with the experimental value of 71.5 meV at $T = 1$ K. Note that the angle of 28° was taken from the previously published neutron diffraction data,[43] acquired at very low temperature (4.2 K), a choice that enables a straightforward comparison of the calculations with the experiment. The origin of the enhancement of T_{N2} is not clear. One possibility is that for a FM layer on the top of a bulk system with zero net magnetization the shape anisotropy would favor an in-plane orientation of the magnetization. A second possibility is that T_{N2} is very sensitive to the magnitude of the B_2^0 and B_4^0 CEF parameters.[44] These CEF parameters might be slightly different for the top Ho-layer than for the bulk.

Conclusion. By studying by ARPES the magnetically active, silicon-terminated surface of $HoRh_2Si_2$ crystals, we have unveiled the spin-dependent properties of the two-dimensional electrons and demonstrated how their energy and spin can be manipulated. The beauty of this system lies in the 4*f* moments, which act as a multiple tuning tool, when their projections parallel and perpendicular to the surface plane order at different temperatures. Together with the RB spin−orbit interaction, this results in effective magnetic fields at the surface with different strength and orientation, which act in competitive ways on the highly mobile itinerant electrons locked within the surface. We found that when the temperature is high and the 4*f*s are disordered, the RB spin−orbit interaction creates an effective magnetic field, which lies exactly within the surface. It locks the spins of the two-dimensional electrons exclusively in the surface plane. A gradual decrease of temperature forces first the 4*f*s component perpendicular to the surface to order. This activates the exchange−magnetic coupling between the 4*f*s and the itinerant surface electrons forcing their spins to be reoriented toward the direction of the ordered 4*f*s. With further decrease of temperature, the 4*f* component parallel to the surface plane becomes ordered. Our experiments disclose how the temperature-dependent competition between fundamental mechanisms such as spin−orbit and magnetic exchange interaction allow to manipulate the spin-dependent properties of electrons by using only one parameter: the temperature. Of particular interest hereby is how the inclination of 4*f* moments and the resulting tilt of effective magnetic fields at the surface act on the two-dimensional electrons in RB systems, which has important implications for possible applications in spintronic devices.

DOI: 10.1021/acs.nanolett.6b04036
Nano Lett. 2017, 17, 811−820

Methods. The temperature dependent ARPES experiments down to 10 K were performed at the Swiss Light Source (SIS X09LA instrument) and at the I05 beamline of the Diamond Light Source (DLS), while temperature range between 10 and 1 K was covered at the "1-cubed ARPES" machine of BESSY-II facility (HZB Berlin). The results measured at different facilities demonstrate a high reproducibility. High quality single-crystalline samples of $HoRh_2Si_2$ were grown by a high-temperature indium-flux method with similar parameters as reported for $GdRh_2Si_2$.[53] To achieve a better visualization of the band-dispersion the data presented in Figure 2a and Figure 4d, they were extracted from the 2D curvature plots[57] of the initial ARPES maps, measured along $\bar{X}-\bar{M}-\bar{X}$ direction at different temperatures. The position of the center of gravity of the spin-spit bands highlighted in Figure 4d by dashed white line was derived from a fit to the experimental data with two Gaussian profiles and a linear background.

Ab initio calculations were performed using the projector augmented-wave method[58] (VASP code[59,60]) within the generalized gradient approximation (GGA) to the exchange-correlation potential.[61] The Hamiltonian containing scalar-relativistic corrections and spin−orbit coupling was taken into account by a second variation procedure.[62] An energy cutoff for the plane-wave expansion of 257.2 eV was used and the two-dimensional Brillouin zone was sampled with a $12 \times 12 \times 1$ k-point mesh. To describe the Ho 4f and Rh 4d states, we used the GGA+U approach[63] within the Dudarev's scheme,[64] in which the effective on-site Coulomb and exchange interaction parameters U and J enter together in the prefactor $U_{eff} = (U - J)/2$ of the correction term of the GGA+U Hamiltonian whereby only the $U - J$ difference is essential. Our test calculations revealed minor variations of the valence band low energy spectra of the bulk $HoRh_2Si_2$ for the values of $U - J = 6$, 7, and 8 eV applied to the strongly correlated Ho 4f states. The value of 7 eV was eventually chosen for the surface band structure calculations as it yielded bulk lattice parameters a = 4.016 Å and c = 9.851 Å almost in perfect agreement with those measured in our experiment (a_{exp} = 4.015 Å and c_{exp} = 9.89 Å). As for the Rh 4d states, a complete set of calculations including a full bulk crystal structure optimization, surface interlayer spacings relaxation and the consecutive surface electronic structure calculations were first performed using a $U - J$ value of 2.9 eV, which has previously led to a good agreement between the calculated and measured surface spectra for the homologue $GdRh_2Si_2$ compound.[46] Taking into account the dominating contribution of the Rh 4d orbitals to the wave functions of the surface states of interest,[45,46] we then treated the $U - J$ value for the Rh 4d states as a parameter varying it in the physically meaningful range to reach a quantitative agreement of the calculated binding energies with those measured by ARPES. The best agreement was found when no $U - J$ correction is applied to the Rh 4d states. Thus, the results presented in Figure 3a and b as well as in the Supplementary Figures S3, S4, and S8 are obtained without additional parameters for the Rh 4d states, but using the crystal structure optimized with $U - J$ = 2.9 eV. To model a paramagnetic state in $HoRh_2Si_2$, the Ho 4f electrons were placed in atomic core. The $HoRh_2Si_2$ (001)-surface was simulated by the 16- and 32-layer-thick asymmetric slabs with the topmost (lowermost) surface terminated by Ho (Si).

■ ASSOCIATED CONTENT

Supporting Information

The Supporting Information is available free of charge on the ACS Publications website at DOI: 10.1021/acs.nanolett.6b04036.

Additional figures with results from model tight-binding and ab initio GGA+U calculations (PDF)

■ AUTHOR INFORMATION

Corresponding Authors

*E-mail: Denis.Vyalikh@tu-dresden.de.

*E-mail: krellner@physik.uni-frankfurt.de.

ORCID

Kristin Kliemt: 0000-0001-7415-4158

Denis V. Vyalikh: 0000-0001-9053-7511

Author Contributions

C.K. and D.V.V. designed the research. K.Kl., C.G., and S.Se. prepared and characterized the samples for spectroscopic experiments. ARPES measurements were done by A.G., A.C., M.G., A.F., S.S., S.D., and D.V.V. Theoretical studies were performed by M.M.O., E.V.C., and M.H. Operation of the ARPES facilities was carried out by M.S., M.R., and N.C.P. at the Swiss Light Source and by Mo.H., P.D., and T.K. at the Diamond Light Source, respectively. The obtained results were discussed together with K.Ku. and C.L. The manuscript was written by A.G., M.M.O., and D.V.V. All authors have read and given approval to the final version of the manuscript.

Notes

The authors declare no competing financial interest.

■ ACKNOWLEDGMENTS

This work was supported by the German Research Foundation (DFG) (Grant Nos. VY64/1-3, GE602/2-1, GRK1621, and SFB1143) as well as by Research Grant No. 15.61.202.2015 of Saint Petersburg State University. We acknowledge Diamond Light Source for beamtime on the beamline I05 under proposal SI11512. The authors acknowledge experimental support from the SIS beamline at Swiss Light Source. The support by the Tomsk State University Academic D.I. Mendeleev Fund Program in 2015 (research grant N 8.1.05.2015), the University of the Basque Country (Grants Nos. GIC07IT36607 and Grant No. IT-756-13), and the Spanish Ministry of Science and Innovation (Grant Nos. FIS2013-48286-C02-02-P and FIS2013-48286-C02-01-P) is also acknowledged.

■ REFERENCES

(1) Žutić, I.; Fabian, J.; Das Sarma, S. Spintronics: Fundamentals and applications. *Rev. Mod. Phys.* **2004**, *76*, 323−410.

(2) Dresselhaus, G. Spin-orbit coupling effects in zinc blende structures. *Phys. Rev.* **1955**, *100*, 580−586.

(3) Rashba, E. Properties of semiconductors with an extremum loop. 1. Cyclotron and combinational resonance in a magnetic field perpendicular to the plane of the loop. *Sov. Phys. Solid State* **1960**, *2*, 1109−1122.

(4) Bychkov, Yu. A.; Rashba, E. I. Properties of a 2D electron gas with lifted spectral degeneracy. *JETP Lett.* **1984**, *39*, 78−81.

(5) Manchon, A.; Koo, H. C.; Nitta, J.; Frolov, S. M.; Duine, R. A. New perspectives for Rashba spin-orbit coupling. *Nat. Mater.* **2015**, *14*, 871−882.

(6) Yan, B.; Stadtmüller, B.; Haag, N.; et al. Topological states on the gold surface. *Nat. Commun.* **2015**, *6*, 10167.

DOI: 10.1021/acs.nanolett.6b04036
Nano Lett. 2017, 17, 811−820

(7) Reinert, F.; Nicolay, G.; Schmidt, S.; Ehm, D.; Hüfner, S. Direct measurements of the L-gap surface states on the (111) face of noble metals by photoelectron spectroscopy. *Phys. Rev. B: Condens. Matter Mater. Phys.* **2001**, *63*, 115415.
(8) Hoesch, M.; Muntwiler, M.; Petrov, V. N.; Hengsberger, M.; Patthey, L.; Shi, M.; Falub, M.; Greber, T.; Osterwalder, J. Spin structure of the Shockley surface state on Au(111). *Phys. Rev. B: Condens. Matter Mater. Phys.* **2004**, *69*, 241401.
(9) Koroteev, Yu. M.; Bihlmayer, G.; Gayone, J. E.; Chulkov, E. V.; Blügel, S.; Echenique, P. M.; Hofmann, Ph. Strong Spin-Orbit Splitting on Bi Surfaces. *Phys. Rev. Lett.* **2004**, *93*, 046403.
(10) Krupin, O.; Bihlmayer, G.; Starke, K.; Gorovikov, S.; Prieto, J. E.; Döbrich, K.; Blügel, S.; Kaindl, G. Rashba effect at magnetic metal surfaces. *Phys. Rev. B: Condens. Matter Mater. Phys.* **2005**, *71*, 201403.
(11) Caviglia, A. D.; Gabay, M.; Gariglio, S.; Reyren, N.; Cancellieri, C.; Triscone, J.-M. Tunable Rashba Spin-Orbit Interaction at Oxide Interfaces. *Phys. Rev. Lett.* **2010**, *104*, 126803.
(12) Banerjee, S.; Erten, O.; Randeria, M. Ferromagnetic exchange, spin−orbit coupling and spiral magnetism at the $LaAlO_3/SrTiO_3$ interface. *Nat. Phys.* **2013**, *9*, 626−630.
(13) Santander-Syro, A. F.; Fortuna, F.; Bareille, C.; Rödel, T. C.; Landolt, G.; Plumb, N. C.; Dil, J. H.; Radović, M. Giant spin splitting of the two-dimensional electron gas at the surface of $SrTiO_3$. *Nat. Mater.* **2014**, *13*, 1085.
(14) McKeown Walker, S.; Riccò, S.; Bruno, F. Y.; et al. Absence of giant spin splitting in the two-dimensional electron liquid at the surface of $SrTiO_3$ (001). *Phys. Rev. B: Condens. Matter Mater. Phys.* **2016**, *93*, 245143.
(15) Ishizaka, K.; Bahramy, M. S.; Murakawa, H.; et al. Giant Rashba-type spin splitting in bulk BiTeI. *Nat. Mater.* **2011**, *10*, 521−526.
(16) Landolt, G.; Eremeev, S. V.; Koroteev, Yu. M.; et al. Disentanglement of Surface and Bulk Rashba Spin Splittings in Noncentrosymmetric BiTeI. *Phys. Rev. Lett.* **2012**, *109*, 116403.
(17) Eremeev, S. V.; Nechaev, I. A.; Koroteev, Yu. M.; Echenique, P. M.; Chulkov, E. V. Ideal Two-Dimensional Electron Systems with a Giant Rashba-Type Spin Splitting in Real Materials: Surfaces of Bismuth Tellurohalides. *Phys. Rev. Lett.* **2012**, *108*, 246802.
(18) Moreschini, L.; et al. Bulk and surface band structure of the new family of semiconductors BiTeX (X = I, Br, Cl). *J. Electron Spectrosc. Relat. Phenom.* **2015**, *201*, 115−120.
(19) Liebmann, M.; et al. Giant Rashba-Type Spin Splitting in Ferroelectric GeTe(111). *Adv. Mater.* **2016**, *28*, 560−565.
(20) Krempaský, J.; Volfová, H.; Muff, S.; et al. Disentangling bulk and surface Rashba effects in ferroelectric α-GeTe. *Phys. Rev. B: Condens. Matter Mater. Phys.* **2016**, *94*, 205111.
(21) Elmers, H. J.; Wallauer, R.; Liebmann, M.; et al. Spin mapping of surface and bulk Rashba states in ferroelectric α-GeTe(111) films. *Phys. Rev. B: Condens. Matter Mater. Phys.* **2016**, *94*, 201403R.
(22) Quay, C. H. L.; Hughes, T. L.; Sulpizio, J. A.; Pfeiffer, L. N.; Baldwin, K. W.; West, K. W.; Goldhaber-Gordon, D.; de Picciotto, R. Observation of a one-dimensional spin-orbit gap in a quantum wire. *Nat. Phys.* **2010**, *6*, 336−339.
(23) Hasan, M. Z.; Kane, C. L. *Colloquium*: Topological insulators. *Rev. Mod. Phys.* **2010**, *82*, 3045−3067.
(24) Carbone, C.; et al. Asymmetric band gaps in a Rashba film system. *Phys. Rev. B: Condens. Matter Mater. Phys.* **2016**, *93*, 125409.
(25) Kane, C. L.; Mele, E. J. Z_2 Topological Order and the Quantum Spin Hall Effect. *Phys. Rev. Lett.* **2005**, *95*, 146802.
(26) Murakami, S. Quantum Spin Hall Effect and Enhanced Magnetic Response by Spin-Orbit Coupling. *Phys. Rev. Lett.* **2006**, *97*, 236805.
(27) König, M.; Wiedmann, S.; Brüne, C.; Roth, A.; Buhmann, H.; Molenkamp, L.; Qi, X. L.; Zhang, S. C. Quantum Spin Hall Insulator State in HgTe Quantum Wells. *Science* **2007**, *318*, 766−770.
(28) Roth, A.; Brüne, C.; Buhmann, H.; Molenkamp, L. W.; Maciejko, J.; Qi, X. L.; Zhang, S. C. Nonlocal Transport in the Quantum Spin Hall State. *Science* **2009**, *325*, 294−297.
(29) Yu, R.; Zhang, W.; Zhang, H. J.; Zhang, S. C.; Dai, X.; Fang, Z. Quantized Anomalous Hall Effect in Magnetic Topological Insulators. *Science* **2010**, *329*, 61−64.
(30) Chang, C.-Z.; et al. Experimental Observation of the Quantum Anomalous Hall Effect in a Magnetic Topological Insulator. *Science* **2013**, *340*, 167−170.
(31) Wei, P.; Katmis, F.; Assaf, B. A.; Hadar, A.; Steinberg, H.; Jarillo-Herrero, P.; Heiman, D.; Moodera, J. S. Exchange-Coupling-Induced Symmetry Breaking in Topological Insulators. *Phys. Rev. Lett.* **2013**, *110*, 186807.
(32) Eremeev, S. V.; Men'shov, V. N.; Tugushev, V. V.; Echenique, P. M.; Chulkov, E. V. Magnetic proximity effect at the three-dimensional topological insulator/magnetic insulator interface. *Phys. Rev. B: Condens. Matter Mater. Phys.* **2013**, *88*, 144430.
(33) Henk, J.; Flieger, M.; Maznichenko, I. V.; Mertig, I.; Ernst, A.; Eremeev, S. V.; Chulkov, E. V. Topological Character and Magnetism of the Dirac State in Mn-Doped Bi_2Te_3. *Phys. Rev. Lett.* **2012**, *109*, 076801.
(34) Qi, X.-L.; Hughes, T. L.; Zhang, S.-C. Topological field theory of time-reversal invariant insulators. *Phys. Rev. B: Condens. Matter Mater. Phys.* **2008**, *78*, 195424.
(35) Cheong, S.-W.; Mostovoy, M. Multiferroics: a magnetic twist for ferroelectricity. *Nat. Mater.* **2007**, *6*, 13−20.
(36) Krempaský, J.; Muff, S.; Bisti, F.; et al. Entanglement and manipulation of the magnetic and spin−orbit order in multiferroic Rashba semiconductors. *Nat. Commun.* **2016**, *7*, 13071.
(37) Baltz, V.; Manchon, A.; Tsoi, M.; Moriyama, T.; Ono, T.; Tserkovnyak, Y. Antiferromagnetism: The next flagship magnetic order for spintronics? *arXiv:cond-mat/1606.04284v1*. arXiv.org e-Print archive. https://arxiv.org/abs/1606.04284 (accessed June 14, 2016).
(38) Hüfner, S. *Photoelectron Spectroscopy. Principles and Applications*; 3rd ed.; Springer-Verlag: Berlin, Heidelberg, NY, 1995.
(39) Jansen, R. Silicon Spintronics. *Nat. Mater.* **2012**, *11*, 400−408.
(40) Jansen, R.; Dash, S. P.; Sharma, S.; Min, B. C. Silicon Spintronics with ferromagnetic tunnel devices. *Semicond. Sci. Technol.* **2012**, *27*, 083001.
(41) Shigeoka, T.; Fujiwara, T.; Munakata, K.; Matsubayashi, K.; Uwatoko, Y. Component-separated magnetic transition in $HoRh_2Si_2$ single crystal. *J. Phys. Conf. Ser.* **2011**, *273*, 012127.
(42) Felner, I.; Nowik, I. Itinerant and local magnetism, superconductivity and mixed valency phenomena in RM_2Si_2 (R = rare earth, M = Rh, Ru). *J. Phys. Chem. Solids* **1984**, *45*, 419−426.
(43) Ślaski, M.; Leciejewicz, J.; Szytuła, A. Magnetic Ordering in $HoRu_2Si_2$, $HoRh_2Si_2$, $TbRh_2Si_2$ and $TbIr_2Si_2$ by Neutron Diffraction. *J. Magn. Magn. Mater.* **1983**, *39*, 268−274.
(44) Takano, Y.; Ohhata, K.; Sekizawa, K. Thermodynamic and Magnetic Properties of $HoRh_2Si_2$: A Comparison between Experiments and Calculations in a Crystal Field Model. *J. Magn. Magn. Mater.* **1987**, *66*, 187−193.
(45) Chikina, A.; et al. Strong ferromagnetism at the surface of an antiferromagnet caused by buried magnetic moments. *Nat. Commun.* **2014**, *5*, 3171.
(46) Güttler, M.; et al. Robust and tunable itinerant ferromagnetism at the silicon surface of the antiferromagnet $GdRh_2Si_2$. *Sci. Rep.* **2016**, *6*, 24254.
(47) Sankar, S. G.; Malik, S. K.; Rao, V. U. S. Crystal Field Effects on the Magnetocrystalline Anisotropy in $HoAl_2$. *J. Solid State Chem.* **1976**, *18*, 303−306.
(48) Jaworska-Gołab, T.; Gondek, L.; Szytula, A.; Zygmunt, A.; Penc, B.; Leciejewicz, J.; Baran, S.; Stüsser, N. Neutron diffraction and magnetization studies of pseudoternary $HoRh_{2-x}Pd_xSi_2$ solid solutions ($0 \leq x < 2$). *J. Phys.: Condens. Matter* **2002**, *14*, 5315−5323.
(49) Winkler, R. *Spin−Orbit Coupling Effects in Two-Dimensional Electron and Hole Systems*; Springer-Verlag: Berlin, Heidelberg, 2003.
(50) Seiro, S.; Geibel, C. Complex and Strongly Anisotropic Magnetism in the Pure Spin System $EuRh_2Si_2$. *J. Phys.: Condens. Matter* **2014**, *26*, 046002.
(51) Shigeoka, T.; Fujiwara, T.; Matsubayashi, K.; Uwatoko, Y. Magnetization processes and phase diagram of $HoRh_2Si_2$ single crystal

DOI: 10.1021/acs.nanolett.6b04036
Nano Lett. 2017, 17, 811−820

having a component-separated magnetic transition. *J. Phys.: Conf. Ser.* **2012**, *391*, 012063.
(52) Shigeoka, T.; Fujiwara, T.; Kondo, A.; Kindo, K.; Uwatoko, Y. High-Field Magnetization Processes of $HoRh_2Si_2$ Single Crystal. *JPS Conf. Proc.* **2013**, *3*, 017005.
(53) Kliemt, K.; Krellner, C. Single crystal growth and characterization of $GdRh_2Si_2$. *J. Cryst. Growth* **2015**, *419*, 37−41.
(54) The 4*f* magnetic moments of Eu^{2+} ($EuRh_2Si_2$) and Gd^{3+} ($GdRh_2Si_2$) are pure spin moments with zero orbital moment. Therefore, there is no first order CEF effect in both compounds, in contrast to the strong CEF effects in $HoRh_2Si_2$. The in-plane ordered moment in $EuRh_2Si_2$ and $GdRh_2Si_2$ thus does not result from CEF effects, but likely from the anisotropy of exchange interactions, since the dipole−dipole interaction would not favor an in-plane moment.
(55) Bychkov, Yu. A.; Mel'nikov, V. I.; Rashba, E. I. Effect of spin−orbit coupling on the energy spectrum of a 2D electron system in a tilted magnetic field. *Sov. Phys. JETP* **1990**, *71*, 401−405.
(56) Getzlaff, M. *Fundamentals of Magnetism*; Springer-Verlag: Berlin, Heidelberg, NY, 2008.
(57) Zhang, P.; Richard, P.; Qian, T.; Xu, Y.-M.; Dai, X.; Ding, H. A precise method for visualizing dispersive features in image plots. *Rev. Sci. Instrum.* **2011**, *82*, 043712.
(58) Blöchl, P. E. Projector augmented-wave method. *Phys. Rev. B: Condens. Matter Mater. Phys.* **1994**, *50*, 17953−17979.
(59) Kresse, G.; Furthmüller, J. Efficient iterative schemes for *ab initio* total-energy calculations using a plane-wave basis set. *Phys. Rev. B: Condens. Matter Mater. Phys.* **1996**, *54*, 11169−11186.
(60) Kresse, G.; Joubert, D. From ultrasoft pseudopotentials to the projector augmented-wave method. *Phys. Rev. B: Condens. Matter Mater. Phys.* **1999**, *59*, 1758−1775.
(61) Perdew, J. P.; Burke, K.; Ernzerhof, M. Generalized Gradient Approximation Made Simple. *Phys. Rev. Lett.* **1996**, *77*, 3865−3868.
(62) Koelling, D. D.; Harmon, B. N. A technique for relativistic spin-polarised calculations. *J. Phys. C: Solid State Phys.* **1977**, *10*, 3107−3114.
(63) Anisimov, V. I.; Zaanen, J.; Andersen, O. K. Band theory and Mott insulators: Hubbard *U* instead of Stoner *I*. *Phys. Rev. B: Condens. Matter Mater. Phys.* **1991**, *44*, 943−954.
(64) Dudarev, S. L.; Botton, G. A.; Savrasov, S. Y.; Humphreys, C. J.; Sutton, A. P. Electron-energy-loss spectra and the structural stability of nickel oxide: An LSDA+U study. *Phys. Rev. B: Condens. Matter Mater. Phys.* **1998**, *57*, 1505−1509.

DOI: 10.1021/acs.nanolett.6b04036
Nano Lett. 2017, 17, 811−820